Check for updates

Dual targeting multiwalled carbon nanotubes for improved neratinib delivery in breast cancer

Amr Selim Abu Lila,[ab] Rohini Bhattacharya,[c] Afrasim Moin,[a] Turki Al Hagbani,[a] Marwa Helmy Abdallah,[ab] Syed Mohd Danish Rizvi,[a] El-Sayed Khafagy,[de] Talib Hussain[f] and Hosahalli Veerabhadrappa Gangadharappa [ID] *[c]

The aim of this study was to develop biotinylated chitosan (Bio–Chi) decorated multi-walled carbon nanotubes (MWCNTs) for breast cancer therapy with the tyrosine kinase inhibitor, neratinib (NT). For achieving such a purpose, carboxylic acid functionalized multiwalled carbon nanotubes (c-MWCNTs) were initially decorated non-covalently with biotin–chitosan (Bio–Chi) coating for achieving a dual targeting mode; pH-dependent release with chitosan and biotin-receptor mediated active targeting with biotin. Afterwards, Bio–Chi decorated c-MWCNTs were loaded with the tyrosine kinase inhibitor, neratinib (NT). The formulation was then characterized by dynamic light scattering, FTIR and EDX. The drug loading efficiency was estimated to be $95.6 \pm 1.2\%$. *In vitro* drug release studies revealed a pH-dependent release of NT from Bio–Chi decorated c-MWCNTs, with a higher drug release under acidic pH conditions. Sulforhodamine B (SRB) cytotoxicity assay of different NT formulations disclosed dose-dependent cytotoxicities against SkBr3 cell line, with a superior cytotoxicity observed with NT-loaded Bio–Chi-coated c-MWCNTs, compared to either free NT or NT-loaded naked c-MWCNTs. The IC_{50} values for free NT, NT-loaded c-MWCNTs and NT-loaded Bio–Chi-coated c-MWCNTs were 548.43 ± 23.1 μg mL^{-1}, 319.55 ± 17.9 μg mL^{-1}, and 257.75 ± 24.5 μg mL^{-1}, respectively. Interestingly, competitive cellular uptake studies revealed that surface decoration of drug-loaded c-MWCNTs with Bio–Chi permitted an enhanced uptake of c-MWCNTs by breast cancer cells, presumably, *via* biotin receptors-mediated endocytosis. To sum up, Bio–Chi-decorated c-MWCNTs might be a promising delivery vehicle for mediating cell-specific drug delivery to breast cancer cells.

1. Introduction

Despite huge efforts to develop novel therapeutic strategies and to promote screening programs to boost early detection, breast cancer remains a leading cause of mortality among women globally.[1–3] Based on the GLOBOCAN estimates of cancer incidence and mortality, the burden of breast cancer is expected to rise to more than 3 million new cases per year, with higher than 1 million annual deaths, by 2040.[4,5] Molecularly, breast cancer has been categorized into five subtypes: luminal A, luminal B,

[a]Department of Pharmaceutics, College of Pharmacy, University of Ha'il, Ha'il 81442, Saudi Arabia

[b]Department of Pharmaceutics and Industrial Pharmacy, Faculty of Pharmacy, Zagazig University, Zagazig 44519, Egypt

[c]Department of Pharmaceutics, JSS College of Pharmacy, JSS Academy of Higher Education and Research, Mysuru 570015, India. E-mail: hvgangadharappa@jssuni.edu.in

[d]Department of Pharmaceutics, College of Pharmacy, Prince Sattam Bin Abdulaziz University, Al-kharj 11942, Saudi Arabia

[e]Department of Pharmaceutics and Industrial Pharmacy, Faculty of Pharmacy, Suez Canal University, Ismailia 41522, Egypt

[f]Department of Pharmacology and Toxicology, College of Pharmacy, University of Ha'il, Ha'il 81442, Saudi Arabia

human epidermal growth factor receptor 2 (HER-2), basal and normal breast like human epidermal growth factor receptor 2. Among them, HER2-positive breast cancer accounts for 25% of all incidences of breast cancer,[6] and is characterized by high malignancy and poor prognosis.[7] Recently, HER-2 receptor, overexpressed on the outer membrane of cancer cells, has been exploited as a key target for molecular therapeutics such as monoclonal antibodies and tyrosine kinase inhibitors.[8,9]

Neratinib (NT) is an irreversible pan-HER tyrosine kinase inhibitor that is used alone[10] or in combination with other chemotherapeutic agents[11] for the treatment of HER2-positive breast cancer. Neratinib binds irreversibly to HER-2 receptor, by targeting a cysteine residue in the ATP binding pocket of the receptor, causing autophosphorylation in cells.[12] In addition, neratinib could efficiently inhibit the downstream signal transduction events and cell cycle regulatory pathway, and thereby, suppresses cancer cell proliferation *via* promoting cell arrest at G1-S (Gap 1/DNA synthesis) phase.[13,14] Nevertheless, despite the promising therapeutic outcomes achieved with molecular therapeutics, including neratinib, a large number of patients relapse as a result of escape mechanisms elicited by HER-2-positive cancer cells.

Nanotechnology is an emerging field of research that strives to overcome the challenges associated with designing and formulation of anticancer drugs. Nanocarrier-based drug delivery systems can offer multiple benefits in treating cancer such as improved bioavailability, targeted delivery, and increased drug stability.[15–18] Among various nanocarriers, carbon nanotubes (CNTs) have significant benefits over conventional drug delivery technologies in the realm of biological applications. The internal cavities of these nanotubes bestow large space for efficient drug loading of many therapeutic agents such as anticancer agents, proteins and nucleic acids. Nevertheless, the expanded use of CNTs in biological systems has been impeded by a variety of toxicity profiles due to their poor dispersion in aqueous medium and/or inefficient uptake by target cells.[19] CNTs are small tubular structures made up of carbon atoms that are arranged to form a honeycomb nanostructure with outstanding physicochemical characteristics.[20] CNTs are often classed as either single-wall carbon nanotubes (SWNTs) or multi-wall carbon nanotubes (MWNTs) based on the number of sheets of carbon atoms. The ready to manipulate surface of CNTs *via* either covalent or non-covalent chemical modification, known as CNT functionalization, bestows CNTs with enhanced water dispersibility, decreased cytotoxicity and enhanced biocompatibility.[21] In addition, CNT functionalization provides extra attachment sites for further drug loading and/or targeting moieties attachment for enhanced biomedical applications.[19,22] Furthermore, when compared to other nanocarriers such as polymeric nanoparticles, liposomes, or dendrimers, studies revealed that CNTs could exert superior drug delivery capability. Carboxylated CNTs, in particular, have a superior *in vitro* and *ex vivo* profiles, as well as a larger drug release capability, particularly at the acidic pH of the tumor microenvironment.[23]

Active targeting approaches have been established to overcome the limitations and permit preferential accumulation of nanocarriers at the target site. The selectivity of ligands to malignant cells avoids harm to noncancerous tissues and guarantees maximum activity of the therapy. Among various targeting ligands, biotin (Bio) has been widely exploited as a targeting moiety to improve cellular uptake of different nanocarrier by tumor cells.[24–26] Biotin receptors are overexpressed in various types of cancers like pancreatic cancer, prostate cancer, ovarian cancer and breast cancer.[26] Chitosan (Chi) is a natural biodegradable polymer that has multifaceted applications in cancer therapy.[27] Its proximal amino group accessible for ligand conjugation, positive charge on its surface allowing electrostatic interaction with negatively charged nanocarriers, along with its tendency to degrade at the acidic pH of tumor microenvironment, all rationalize chitosan use in pharmaceutical formulation.

In this study, we aimed at developing a dual targeted nanoformulation for the tyrosine kinase inhibitor, neratinib. Carboxylated MWCNTs were initially functionalized with a polymer blend of biotin and chitosan (Bio–Chi) in order to ensure site-specific targeting. Biotin provides receptor mediated drug release, while chitosan provides pH dependent drug release. Then the drug was loaded. Finally, the developed formulation was physico-chemically characterized and the *in vitro* cytotoxicity of NT-loaded c-MWCNTs was assessed against breast cancer cells.

2. Materials and methods

2.1. Materials

Neratinib (NT) was obtained from Beijing Mesochem Technology Co. (Beijing, China). Carboxylic acid functionalized multiwalled carbon nanotubes (>8% carboxylic acid functionalized, average diameter 9.5 nm, 1.5 μm length) were procured from Merck Life Science Private Limited (Mumbai, India). Biotin was obtained from HIMEDIA (Mumbai, India). Chitosan (molecular weight 50 000–190 000 Da, 75–85% deacetylated) was provided by NP CHEM (Mumbai, India). 1-Ethyl-3-(3-methylaminopropyl)carbodiimide (EDC), MTT reagent (3-(4,5-dimethylthiazol-2-yl)-2,5-diphenyl tetrazolium bromide), and *N*-hydroxysuccinimide were purchased from Sigma-Aldrich (St. Louis, MO, USA).

2.2. Preparation of formulation

2.2.1. Preparation of biotinylated chitosan (Bio–Chi) complex. Biotinylated-chitosan was prepared by adding 230 mg of biotin and 160 mg of 1-ethyl-3-(3-methylaminopropyl) carbodiimide (EDC) in anhydrous dimethyl sulfoxide (DMSO). The solution was continuously stirred for 60 min at 25 °C. In another beaker, 400 mg of chitosan were dissolved in sodium acetate buffer (pH 4.5). Both the solutions are mixed and stirred for 24 h. The mixture was then filtered, and the obtained biotinylated chitosan (Bio–Chi) complex was stored at 5 °C.[28]

2.2.2. Conjugation of Bio–Chi with c-MWCNT. In order to conjugate the c-MWCNT to Bio–Chi complex, the carboxylic acid groups present on the surface of c-MWCNT were activated. To activate the carboxylic groups, c-MWCNT were dispersed into 10 mL phosphate buffer (pH 5.0) containing 100 mg of EDC and *N*-hydroxysuccinimide (NHS) (2 : 1 ratio (w/w)). 100 mg of Bio–Chi complex was then added to the above suspension and continuously stirred for 24 h at room temperature until the reaction is completed. Finally, centrifugation (Remi R-8C, Electrotechnik Ltd, India) was applied to remove the excess of coupling reagent. The obtained polymer coated c-MWCNT was filtered and dried at room temperature. Energy dispersive X-ray (EDX) analysis was carried out to confirm the conjugation of Bio–Chi complex to c-MWCNTs.[29]

2.2.3. Loading of drug into Bio–Chi–c-MWCNT. An ethanolic solution of neratinib (NT) was prepared by adding 5 mg of NT in 5 mL ethanol. 6 mg of Bio–Chi–c-MWCNT was added to the solution. The mixture was then sonicated for 30 min using bath sonicator (Julabo Labortechnik GMBH, Seelbach, Germany) for loading of NT to Bio–Chi–c-MWCNT, followed by stirring 15 h at 25 °C. The resultant solution was centrifuged at 9000 rpm for 10 min at 25 °C (Remi R-8C, Electrotechnik Ltd, India). Product was filtered using Whatman filter paper and washed with excess of ethanol. The produced polymer coated neratinib-loaded multiwalled carbon nanotubes (Bio–Chi–c-

MWCNT–NT) was then dried at 30 °C and stored in desiccator at room temperature.[30]

2.3. Characterization of Bio–Chi–c-MWCNT–NT

2.3.1. Drug loading efficiency. The percentage drug loading efficiency of NT within polymer coated c-MWCNT was assessed by indirect method. Briefly, after separating the produced drug-loaded c-MWCNT by centrifugation, the free un-encapsulated drug in the supernatant was quantified spectrophotometrically at 260 nm by UV-visible spectrophotometer (Shimadzu-1800, Tokyo, Japan).[31] The percentage drug loading efficiency was calculated by the following formula:

$$\% \ \text{Drug loading efficiency} =$$

$$\frac{\text{amount of initial drug} - \text{amount of free drug}}{\text{amount of initial drug}} \times 100$$

2.3.2. Particle size distribution and zeta potential measurements. The size and zeta potential of naked carboxylic acid functionalized multiwalled carbon nanotubes (c-MWCNT), and NT-loaded Bio–Chi-coated c-MWCNTs formulation were estimated adopting a photon correlation spectrometer Zetasizer Nano ZS Malvern Instruments (Worcestershire, UK). Measurements were conducted in distilled water at 25 °C, and the samples were read in triplicate.

2.3.3. Transmission electron microscopy (TEM) analysis. Transmission electron microscopy (TEM) image of CNTs were obtained by drop-coating MWCNTs suspension on carbon-coated copper grids. Prior to measurement, the films on the TEM grids were allowed to dry. The TEM measurements were performed using Jeol/JEM 2100 microscope (JEOL Ltd, Tokyo, Japan).

2.3.4. Fourier transformed infrared spectroscopy (FT-IR). FT-IR analysis was conducted to detect the compatibility between drug and polymers, and to detect presence of multiple components in the formulation. The formation of chemical bonds due to the interaction of functional groups was confirmed by FT-IR analysis. In order to reduce the moisture content and to increase the signal level, the detector was purged with clean and dry helium gas. The pure samples of biotinylated chitosan (Bio–Chi), carboxylic acid functionalized multiwalled carbon nanotubes (c-MWCNT), neratinib (NT) and NT-loaded Bio–Chi-coated c-MWCNTs formulation were analyzed by FT-IR 8400S Shimadzu spectrophotometer (Kyoto, Japan). The samples for analysis were prepared as pellets along with KBr. The range of wavelength selected was 400–4000 cm^{-1}.[32]

2.3.5. ¹H-Nuclear magnetic resonance. The instrument used for recording the ^{1}H NMR spectrum was Agilent 400 MHz FT-NMR spectrophotometer (Agilent Scientific Instruments, Santa Clara, CA, USA) operating at 400 MHz for protons. Samples (6 mg mL^{-1}) were first dissolved in CDCl$_3$ by keeping it at 50 °C overnight followed by vortex mixing for several minutes. With the deuterated solvent *i.e.*, CDCl$_3$, the sample was scanned in the NMR tubes using tetramethylsilane as an internal standard.

2.4. *In vitro* drug release

The *in vitro* NT release pattern from c-MWCNT was assessed at two different pH conditions: pH 7.4 (phosphate buffer) and pH 5 (acetate buffer) to simulate the physiological and cancerous pH, respectively. An aqueous dispersion of 2 mg mL^{-1} of formulation was loaded into the dialysis tubing (12–14 kDa molecular weight cut-off (MWCO)) and suspended into the container holding 200 mL dialysis medium, stirred for 72 h at 37 ± 0.5 °C at 100 rpm. 2 mL samples were collected at periodic interval up to 72 h and absorbance was checked using UV-visible spectrophotometer at 260 nm.

2.5. *In vitro* cytotoxicity study

2.5.1. Cell culture. Noncancerous MCF10A human mammary epithelial cell line, triple negative breast cancer MDA-MB-231 cell line, and HER2-positive SkBr3 breast cancer cell line was obtained from National Centre for Cell Science (NCCS), Pune, India. All cell lines were maintained in Dulbecco's Modified Eagle Medium (DMEM; Hi-Media Lab, Mumbai, India) nourished with 10% fetal bovine serum, and 0.5 mg mL^{-1} penicillin–streptomycin (Gibco Life Technologies, Gaithersburg, MD, USA) and incubated at 37 °C and 5% CO$_2$.

2.5.2. *In vitro* cytotoxicity assessment using sulforhodamine B (SRB) assay. SRB assay was utilized to examine the *in vitro* cytotoxicity of the formulation against different cell lines.[33] Briefly, 1×10^4 cells per well were plated in a 96-well plate for 24 h. The cells were treated with serial dilutions of free NT, NT-loaded c-MWCNTs or NT-loaded Bio–Chi-coated c-MWCNTs formulation in triplicates (1000, 500, 250, 125, 62.5 and 31.25 μg mL^{-1}). Untreated cells were served as a control. Following the treatment, the plate was incubated at 37 °C with 5% CO$_2$ for 48 h. At the end of incubation period, 50 μL of ice-cold 10% (w/v) trichloro acetate (TCA) was added into each well and the plates were incubated at 40 °C for 1 h to fix the cells. Next, the plates were rinsed four times, and 100 μL of 0.4% SRB solution (prepared in 1% acetic acid) was added to each well and the plates were left at room temperature for 30 min. Following the incubation, the plates were rinsed with 1% acetic acid and the excess solution was eliminated by snapping the plates on absorbent paper. 100 μL of 10 mM tris base solution was added to each well. The plates were gently tapped to dissolve the bound SRB and the optical density of the pink solution in the plates was recorded by a multimode plate reader (EnSpire 2300, PerkinElmer, Waltham, MA, USA) at 510 nm. The percentage of inhibition was estimated using the formula:

$$\% \ \text{Cytotoxicity} = \frac{\text{OD}_{\text{control}} - \text{OD}_{\text{sample}}}{\text{OD}_{\text{control}}} \times 100$$

2.5.3. Cell uptake studies. To examine the intracellular uptake of formulation by fluorescent microscope, Bio–Chi–c-MWCNT–NT was tagged by the fluorescence probe fluorescein isothiocyanate (FITC). Briefly, a fresh solution of 1 mg mL^{-1} of FITC was prepared by dissolving 1 mg of FITC in 1 mL dimethyl sulfoxide (DMSO). This solution was then reacted with Bio–Chi–c-MWCNT–NT in a ratio of 1 : 10 at 4 °C for 12 h. The mixture

was dialyzed against ultrapure water for 24 h to generate FITC labeled Bio–Chi–c-MWCNT–NT. The unbound FITC was removed by dialysis using water in the dialysis tubing.

To investigate the possible contribution of biotin receptor to the enhanced the cellular uptake of NT-loaded Bio–Chi-coated c-MWCNTs by cancer cells, a competitive cellular uptake experiments in presence of free biotin was conducted. Initially, 1×10^5 SkBr3 cells were plated in a six well plate with cover slip and incubated for 24 h. The cells were then incubated in the presence or absence of 2 mM free biotin for 2 h before treatment with Bio–Chi-coated c-MWCNTs. Afterwards, the medium is replaced with fresh media containing Bio–Chi-coated c-MWCNTs and the cells were further incubated for 4 h at 37 °C. After aspirating the supernatant, the cells were fixed with formaldehyde solution. The coverslips were then placed onto slides with mounting solution containing DAPI. The cell uptake of formulation was evaluated with florescent microscope.

2.6. Statistical analysis

Statistical analysis was performed using t-test and one way analysis variance (ANOVA) employing the GraphPad Prism 6.0 software. A p value less than 0.05 indicates a significant difference.

3. Results and discussion

3.1. Synthesis of biotinylated-chitosan coated NT-loaded MWCNTs (Bio–Chi–c-MWCNT–NT)

Carbon nanotubes (CNTs) have attracted the interest of many researchers owing to their multifunctional application potential in cancer therapy and diagnosis.[34–36] In this study, MWCNTs functionalized with carboxylic groups (c-MWCNTs), with enhanced aqueous dispersibility, were initially decorated with a polymer blend of biotin and chitosan (Bio–Chi) in order to ensure site-specific targeting. Energy dispersive X-ray (EDX) spectroscopy was carried out to affirm the conjugation of Bio–Chi to c-MWCNTs. The existence of a prominent sulphur peak in the EDX spectra of c-MWCNTs (Fig. 1), corresponding to biotin, strongly confirmed the successful conjugation/coating
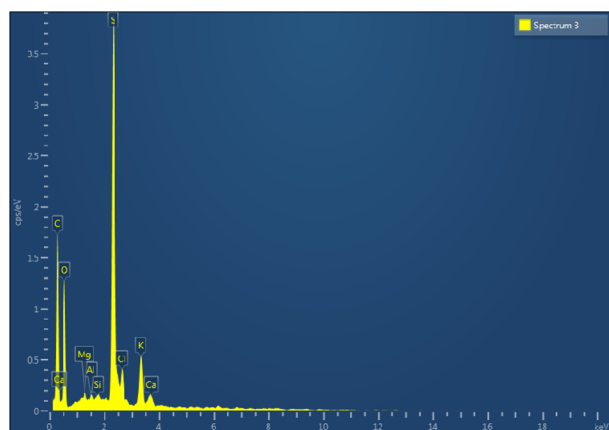
of targeting ligands (biotinylated chitosan) onto the surface of c-MWCNTs. Eventually, surfaces modified c-MWCNTs were loaded with the pan-HER tyrosine kinase inhibitor, neratinib (NT). Fig. 2 depicts a schematic representation of biotinylated-chitosan coated NT-loaded MWCNTs (Bio–Chi–c-MWCNT–NT) synthesis process.

3.2. Characterization of synthesized Bio–Chi–c-MWCNT–NT

3.2.1. Drug entrapment efficiency and drug loading percentage. The unique structure of CNTs holds numerous merits over other nano-sized delivery vehicles, particularly, an exceptionally high drug loading efficiency. In this study, sonication was adopted to physically load NT onto c-MWCNTs from a saturated ethanolic solution of NT. The percent drug loading efficiency was found to be $95.6 \pm 1.2\%$. The relatively high entrapment efficiency confirms the effectiveness of the preparation method in attaining high drug loading within c-MWCNTs.

3.2.2. Particle size and zeta potential measurement. The sizes and zeta potential of naked c-MWCNTs and Bio–Chi-coated drug loaded c-MWCNTs were characterized using a dynamic light scattering instrument (Table 1). The particle size of naked c-MWCNTs was 218.5 ± 11.2 nm. The size of drug-loaded polymer coated c-MWCNTs increased to 285.9 ± 13.4 nm, presumably, due to the efficient conjugation of Bio–Chi coating to c-MWCNTs.

The surface charge of the c-MWCNT was also assessed at various stages; before and after polymer coating of c-MWCNTs (Table 1). Plain c-MWNTs showed a net negative zeta potential value of -20.4 ± 2.1 mV, presumably due to surface functionalization with carboxylic acid groups. Interestingly, the zeta potential of polymer coated drug-loaded c-MWCNTs changed to $+11.3 \pm 1.8$ mV, presumably, due to the coating with the positively charged chitosan.[37] Such change in zeta potential clearly
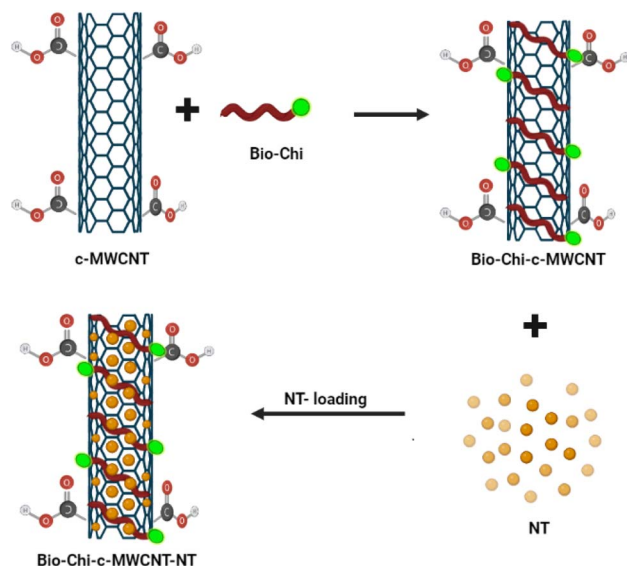

Fig. 1 EDX of Bio–Chi–c-MWCNT–NT.

Fig. 2 Overview of drug loading into the c-MWCNT and polymer coating.

Table 1 Particle size, polydispersity index (PDI), and zeta potential of naked c-MWCNTs and Bio–Chi-coated c-MWCNTs–NT ($n = 3$)

Formulation	Particle size (nm)	PDI	Zeta potential (mV)
c-MWCNT	218.5 ± 11.2	0.269	–20.4 ± 2.1
Bio–Chi–c-MWCNT–NT	285.9 ± 13.4	0.205	+11.3 ± 1.8

suggest the efficient polymer coating of drug-loaded c-MWCNT with Bio–Chi coating.

3.2.3. TEM analysis. The MWCNT sample size and surface morphology were examined using transmission electron microscopy (TEM). Fig. 3 shows the typical TEM image of naked MWCNTs and Bio–Chi–c-MWCNT–NT. As depicted in Fig. 3A, naked MWCNTs were found to be homogenous with a mean diameter of 10–20 nm. Fig. 3B represents the image of MWCNTs after polymer coating. The surface of polymer coated MWCNTs has become rough, probably, due to polymer coating. In addition, small spherical particles were observed on the side walls of the CNTs, suggesting the efficient entrapment of NT.

3.2.4. Fourier transformed infrared spectroscopy (FT-IR). FT-IR spectra of c-MWCNT, pure NT, Bio–Chi and Bio–Chi–c-MWCNT–NT were investigated to affirm the efficient loading of NT onto c-MWCNTs (Fig. 4). The FTIR spectra of c-MWCNTs clearly depicts the functional groups on the surface of the c-MWCNTs. The characteristic peak at 1628 cm^{-1} is related C=O. Observed peaks at 2856 and 3433 cm^{-1} are related to C–H stretching bonds and O–H (carboxylic acid) group, respectively.[38] The spectra of NT exhibited distinct absorption peaks at 3427 cm^{-1} (for N–H stretching vibrations); 3034 cm^{-1} (for C–H stretching vibrations); 2204 cm^{-1} (for C≡N stretching vibrations); 1622 cm^{-1} (for C=O stretching vibrations).[39] The spectra of Bio–Chi showed distinct peaks at 3360; 3308 and 2928 cm^{-1} corresponding to the stretching vibration of O–H and N–H, and C–H, respectively. The peak at 1641 cm^{-1} indicates the bending amide bond formed between biotin and chitosan, suggested the possibility of a strong interaction between Bio and Chi.[40] Most importantly, in the spectra of drug loaded c-MWCNTs, all the peaks corresponding to the drug were observed with no significant changes, indicating efficient drug loading and the absence of any specific chemical interaction between the CNTs and drug.
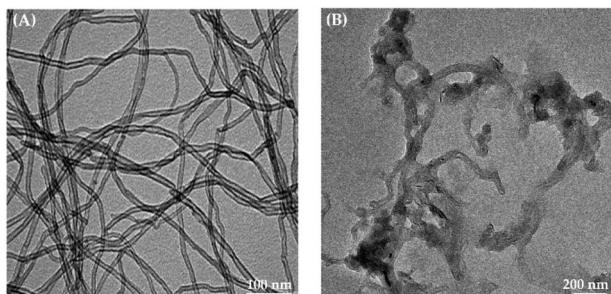

Fig. 3 TEM images of (A) naked MWCNTs, and (B) Bio–Chi–c-MWCNT–NT.

3.2.5. ¹H-Nuclear magnetic resonance (¹H-NMR). In order to confirm the appropriate synthesis of Bio–Chi–c-MWCNTs–NT, ¹H-NMR analysis was conducted. As depicted in Fig. 5, the ¹H-NMR spectrum of Bio–Chi–c-MWCNT–NT showed characteristic signals between 6.73 and 8.89 ppm, revealing the presence of aromatic protons of neratinib. In addition, the peaks appeared between 3.90 ppm and 4.29 ppm represent protons adjacent to heterocyclic atom (N–CH$_3$ protons) and those of amine group present in neratinib. Of interest, the presence of a distinct peak at 6.03 ppm indicates the presence of amide protons, which confirms successful conjugation of Bio–Chi and c-MWCNTs. Furthermore, the presence of peaks at 9.60 ppm and 9.7 ppm might reveal the presence of carboxylic acid (COOH) groups related to biotin and c-MWCNT. These peaks showed an up-fielding effect due to electron shielding. Of note, the peaks at 2.46, 2.75 and 3.30 ppm should be neglected as they are corresponding to DMSO.[41]

3.3. *In vitro* drug release

The *in vitro* release profile of NT from Bio–Chi–c-MWCNT–NT was examined at two pH conditions: pH 5 and pH 7.4, corresponding to the lysosomal pH and physiological pH values, respectively, for 72 h. As depicted in Fig. 6, NT released slowly from Bio–Chi–c-MWCNT–NT in PBS of pH 7.4, with about 60% of the loaded drug released at 72 h. In contrast, drug release was remarkably enhanced at pH 5, with more than 90% of the entrapped drug released at the same time interval. This pH-dependent drug release from Bio–Chi–c-MWCNTs might be ascribed to the pH sensitivity of c-MWCNTs polymer coating (Bio–Chi). It is well known that chitosan is readily soluble in dilute acidic medium below pH = 6.5,[42] accordingly, at lower pH values (pH 5), chitosan would readily dissolve and provide a naked system of c-MWCNT loaded with NT, which permit higher drug release at pH 5, compared to pH 7.4. Similar results were reported by Khoshoei *et al.*[43] who emphasized the potential role trimethyl chitosan grafted onto the surface of CNTs in facilitating the release of entrapped doxorubicin at acidic environment of tumor tissue. Collectively, these findings imply that c-MWCNTs, with their pH-sensitive drug release capabilities and high drug loading efficiency, might be promising cancer therapeutic delivery vehicles. Where, the entrapped drug will be retained within Bio–Chi-coated c-MWCNTs during its transient in neutral blood conditions, while, at the low pH of the cancer environment, Bio–Chi coating will dissolve allowing quick drug release from naked c-MWCNTs in a controlled manner, sparing healthy tissues from the drug-related deleterious effects.

3.4. *In vitro* cytotoxicity of Bio–Chi-coated c-MWCNTs–NT

The sulforhodamine B (SRB) test is used to determine cell density by measuring cellular protein concentration.[44] This approach was utilized herein for screening cellular toxicity of NT-loaded c-MWCNTs against SkBr3 breast cancer cells (Fig. 7). In this study, SkBr3 cells were treated with serial dilutions of either free NT, NT-loaded c-MWCNTs or NT-loaded Bio–Chi-coated c-MWCNTs and the *in vitro* cell viability was assessed
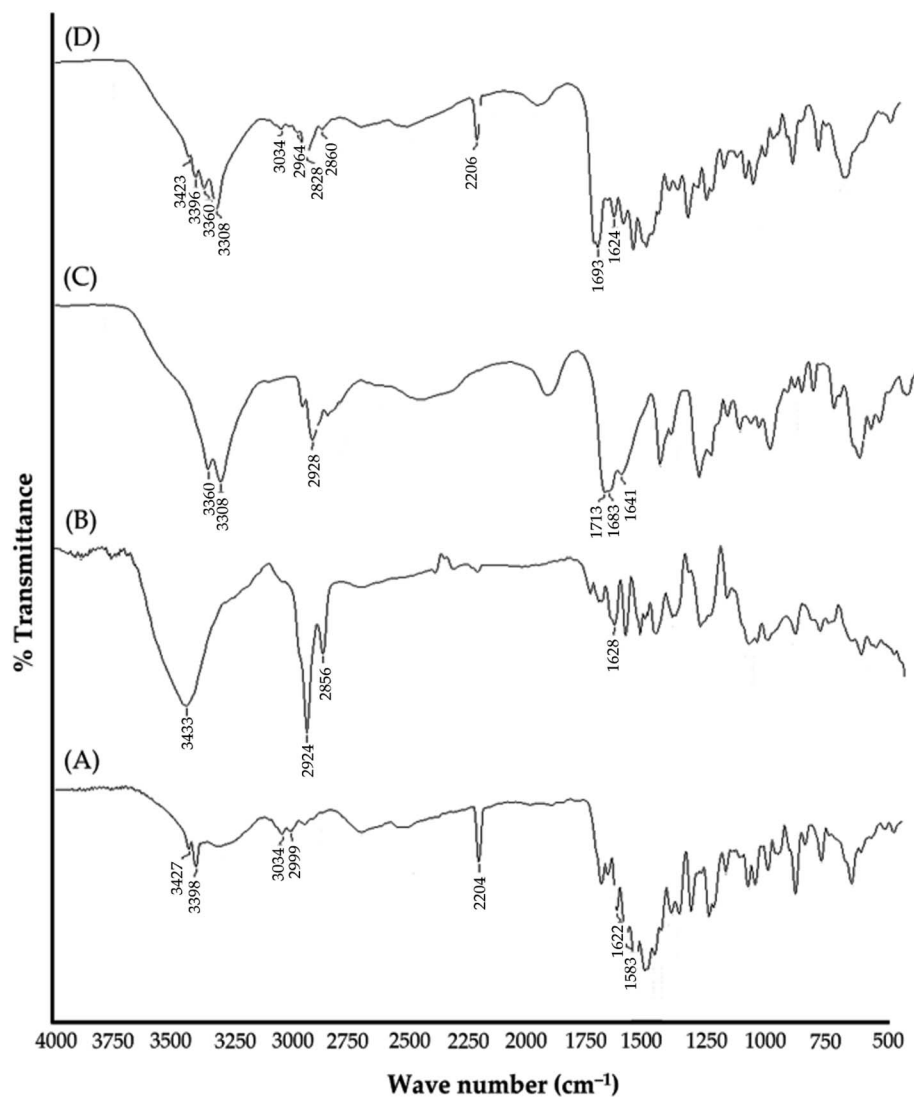
Fig. 4 FT-IR spectra of (A) NT, (B) c-MWCNT, (C) Bio–Chi, and (D) Bio–Chi–c-MWCNT–NT.

at 48 h post incubation. Fig. 7 depicts the *in vitro* cytotoxicity of several NT formulations. Blank Bio–Chi–c-MWCNTs did not exert a notable cytotoxic impact on SkBr3 cells, causing less than 20% cell death after 48 h of incubation with 1000 µg mL^{-1} of CNTs (Fig. 7). On the other hand, all tested NT formulations exerted a dose-dependent cytotoxicity against SkBr3 cells. Of interest, NT-loaded Bio–Chi–c-MWCNTs showed a superior cytotoxic effect against SkBr3 cells, compared to either free NT or NT-loaded c-MWCNTs. The cell viability treated with free NT, NT-loaded c-MWCNTs or NT-loaded Bio–Chi-coated c-MWCNTs was $40.1 \pm 2.3\%$, $32.1 \pm 2.6\%$, and $18.5 \pm 1.9\%$, respectively, upon treatment with 1000 µg mL^{-1} of drug for 48 h. Furthermore, the calculated IC$_{50}$ values for free NT, NT-loaded c-MWCNTs or NT-loaded Bio–Chi-coated c-MWCNTs were in the following order 548.43 ± 23.1 µg mL^{-1}, 319.55 ± 17.9 µg mL^{-1}, and 257.75 ± 24.5 µg mL^{-1}, respectively. The superior cytotoxic effect of NT-loaded Bio–Chi-coated c-MWCNTs, compared to either free NT or NT-loaded c-MWCNTs could be ascribed to the preferential intracellular delivery of NT to cancer cells *via* biotin receptor-mediated cellular internalization of drug-loaded c-MWCNTs. Similar results were reported by Badea *et al.*[45] who underscored the potential of carboxyl-functionalized carbon nanotubes for enhancing the cytotoxic potential of cisplatin against breast cancer cells compared to free cisplatin.

Neratinib has also been reported to exert a remarkable cytotoxic effect against not only HER2-positive breast cancer cells but triple-negative breast cancer cells as well.[44] Consequently, in this study the cytotoxic potential of polymer coated NT-loaded c-MWCNT was examined against triple-negative MDA-MB 231 breast cancer cells (Fig. 8). As depicted in Fig. 8, Bio–Chi-coated NT-loaded c-MWCNT could exert a pronounced cytotoxic effect against MDA-MB 231, but at relatively higher concentrations. The cell viability of MDA-MB 231 cells was reduced by $\sim$50% upon treatment with 1000 µg mL^{-1} Bio–Chi-coated NT-loaded c-MWCNT. The estimated IC$_{50}$ of Bio–Chi-coated NT-loaded c-MWCNT against MDA-MB 231 cells was 1496.12 ± 101.7 µg mL^{-1}, which is $\sim$6 folds higher than that observed with HER2-positive SkBr3 cells. These results the
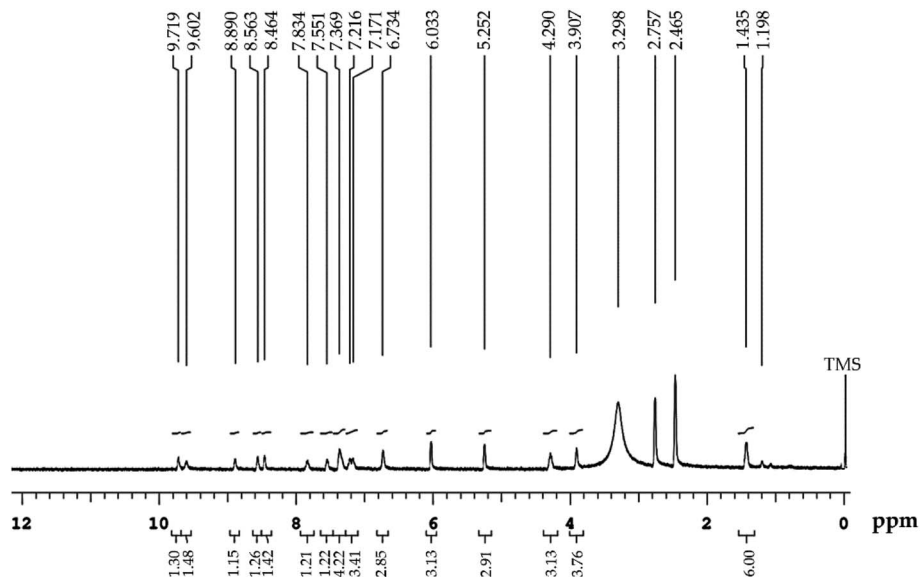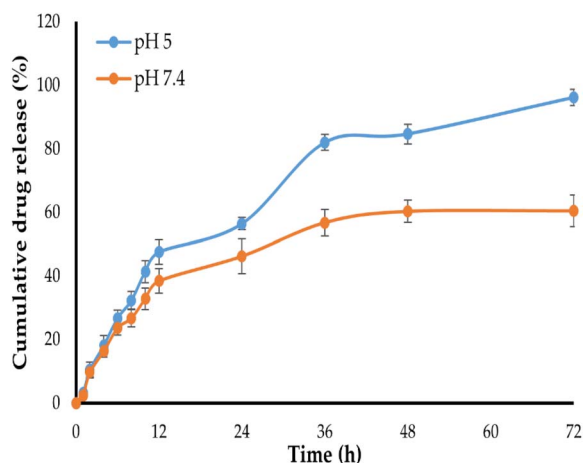

Fig. 5 ^{1}H-NMR data of Bio–Chi–c-MWCNTs–NT.

Fig. 6 *In vitro* release profile of Bio–Chi–c-MWCNT–NT at pH 5 and pH 7.4.

verify whether surface coating of c-MWCNTs with biotinylated chitosan polymer could contribute to the superior cytotoxicity of NT-loaded Bio–Chi–c-MWCNTs, Bio–Chi-coated c-MWCNTs were tagged with a fluorescent probe, fluorescein iso-thiocyanate (FITC), and the cellular uptake of NT-loaded Bio–Chi-coated c-MWCNTs by SkBr3 cancer cells was traced in the presence and/or absence of free biotin by a fluorescence microscope. As demonstrated in Fig. 9, pretreatment with free biotin (2 mM) remarkably inhibited the cellular uptake of biotin-coated c-MWCNTs by SkBr3 cells as displayed by the absence of fluorescence signals (Fig. 9B), which obviously indicates that free biotin could hunk the binding and/or uptake of biotin-coated c-MWCNTs with biotin receptors expressed at the surface of cancer cells. Furthermore, the extent of cellular uptake of c-MWCNTs in terms of mean fluorescence intensity (MFI), was quantitatively determined. Significantly higher
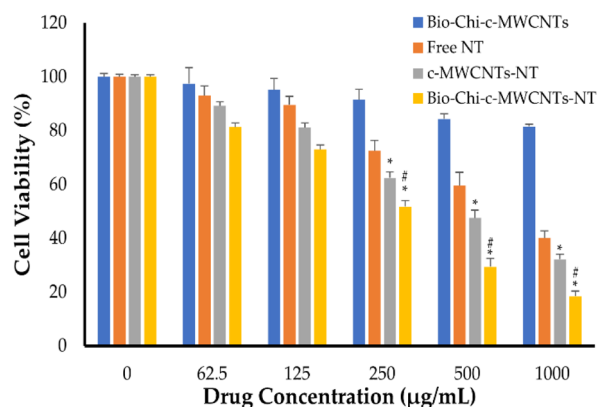
higher selectivity of Bio–Chi-coated NT-loaded c-MWCNT against HER2-positive SkBr3 cells, compared to triple-negative MDA-MB 231 breast cancer cells.

Finally, in order to address the safety of polymer coated NT-loaded c-MWCNT against noncancerous cells, normal MCF10A human mammary epithelial cells were treated with various concentrations of drug-loaded c-MWCNTs. As evident in Fig. 8, drug-loaded c-MWCNTs failed to exert notable cytotoxic effects against MCF10A cells under the tested concentrations; with ~85% of the cells were viable upon treatment with 1000 μg mL^{-1} Bio–Chi-coated NT-loaded c-MWCNT. These results suggest the safety of c-MWCNT formulation against noncancerous cells.

3.5. Cellular uptake of NT-loaded Bio–Chi-coated c-MWCNTs

Cellular uptake is a critical step that dictates the cytotoxic effi-cacy of anticancer drugs against cancerous cells. Accordingly, to

Fig. 7 *In vitro* cytotoxicity of Bio–Chi-coated NT-loaded c-MWCNT. (A) Cell viability of SkBr3 cells treated with either Bio–Chi–c-MWCNTs, free NT, NT-loaded c-MWCNTs, or NT-loaded Bio–Chi–c-MWCNTs. *$p < 0.5$ *vs.* free NT and $^\#p < 0.05$ *vs.* c-MWCNTs–NT.
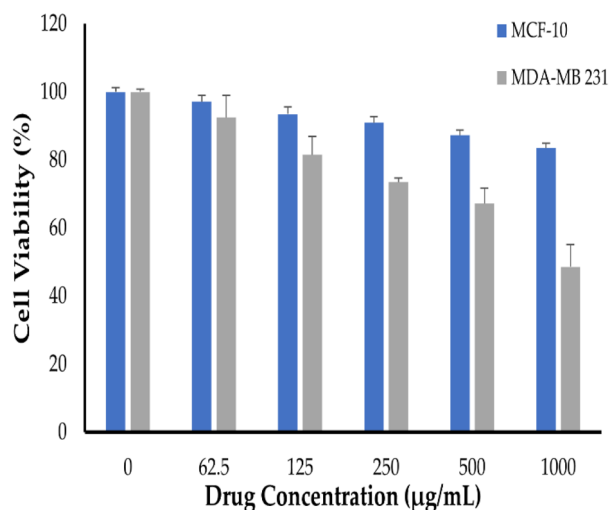
Fig. 8 *In vitro* cell viability of triple-negative MDA-MB 231 breast cancer cells and normal MCF10A human mammary epithelial cells treated with NT-loaded Bio–Chi–c–MWCNTs.

fluorescence intensity ($p < 0.5$) was observed in SkBr3 cells treated with biotin-coated c-MWCNTs in the absence of the competitive inhibitor, free biotin, compared to those treated with biotin-coated c-MWCNTs in the presence of free biotin

(Fig. 9C). Collectively, these findings proved that the presence of free biotin hindered cellular uptake of biotin-coated c-MWCNTs and that biotin-coated c-MWCNTs are mainly taken up the breast cancer cells *via* the biotin receptor.

The application of nanotechnology to carbon-based materials has led to the development of a variety of nanostructures, including carbon-based nanoribbons, quantum dots, nanowires, … *etc.*[46–48] Among them, CNTs have been emerged as a promising nano-delivery vehicle that have significant several advantages over conventional drug delivery technologies in the realm of biological applications. The huge internal cavities of these nanotubes can afford efficient drug loading of many therapeutic entities such as anticancer drugs.[34] In addition, because of its unique architecture, a variety of bioactive compounds may be immobilized (non-covalently or covalently) on the CNT's exterior surface for achieving active drug targeting.[49–51] Furthermore, the tubular shape of CNTs at the microscopic level allows them to pierce cell membranes like a needle without triggering morphological cell alterations or death.[52] In this study, c-MWCNTs, with enhanced aqueous dispersion properties, were challenged as a delivery vehicle for cancer therapy. The external surface of c-MWCNTs was decorated with biotin–chitosan polymer to ensure efficient targeting ability.[53] Our results suggest three key steps participating in the nanotube-based drug delivery system. First, NT-loaded Bio–Chi c-MWCNTs are initially attached to the cell membrane of breast
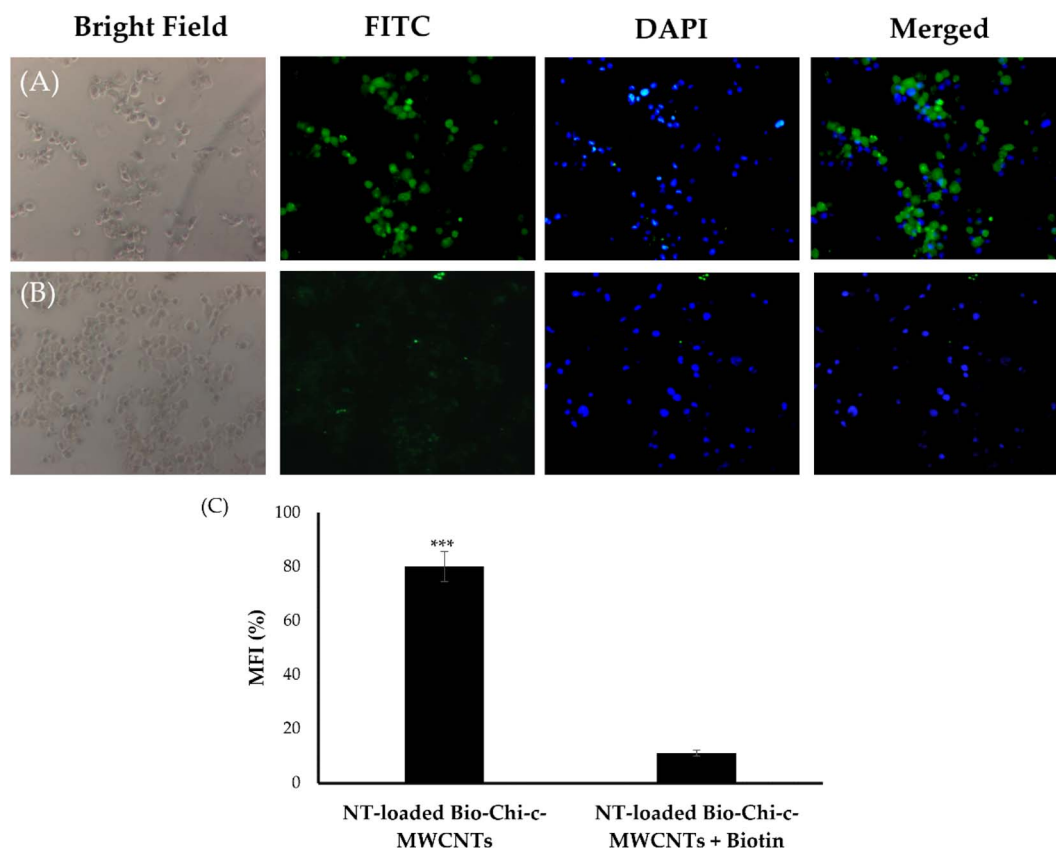

Fig. 9 Cellular uptake of NT-loaded Bio–Chi–c–MWCNTs by SkBr3 breast cancer cells in (A) absence or (B) presence of 2 mM free biotin. (C) Quantification of mean fluorescence intensity (MFI) percentage. ***$p < 0.001$.

cancer cell lines *via* biotin targeting ligand followed by cellular uptake of c-MWCNTs by biotin receptor-mediated endocytosis (Fig. 9). Second, upon internalization, NT is readily released at the lysosomal acidic pH (Fig. 6). Finally, the adequately released drug exerts its cytotoxic effect against cancer cells (Fig. 7). To the best of our knowledge, this is the first study to emphasize the potential of biotin-decorated c-MWCNTs as a delivery vehicle for NT targeting to breast cancer cells. Nevertheless, *in vivo* model-based exploratory studies interpreting the efficacy and/or safety of NT-loaded Bio–Chi c-MWCNTs are still a necessity to fully substantiate the efficacy Bio–Chi c-MWCNTs as a delivery vehicle in breast cancer therapy.

4. Conclusions

The dual targeted drug delivery based on c-MWCNT encapsulated with anti-cancer drug, NT, was successfully formulated for breast cancer therapy. NT was efficiently loaded within c-MWCNTs as manifested by high entrapment efficiency percent (>95%). EDX analysis confirmed the efficient decoration of drug-loaded c-MWCNTs with Bio–Chi coating. The *in vitro* release study emphasized pH-dependent drug release from Bio–Chi functionalized c-MWCNTs. Cellular uptake studies clearly implied the role of Bio–Chi coating in improving the target-ability of drug-loaded c-MWCNTs against breast cancer cells *via* promoting biotin receptor-mediated internalization of c-MWCNTs within cancer cells, with subsequent induction of potent cytotoxic effect. To summarize, c-MWCNTs with the targeting moiety, Bio–Chi, might be a potential platform for anticancer treatment. Nevertheless, a thorough knowledge of the *in vivo* fate and/or safety profile of c-MWCNTs is critically required before their adoption in clinical settings.

Author contributions

Conceptualization, A. S. A., T. A. and M. H. A.; methodology, R. B., H. V. G., A. M., S. M. D. R., and T. H.; software, E.-S. K., T. A. and M. H. A.; validation, A. S. A. and A. M.; formal analysis, E.-S. K. and T. H.; investigation, H. V. G., A. M., S. M. D. R., and T. H.; writing—original draft preparation, H. V. G., E.-S. K., T. A. and M. H. A.; writing—review and editing, A. S. A.; supervision, H. V. G.; project administration, A. S. A.; funding acquisition, A. S. A. All authors have read and agreed to the published version of the manuscript.

Conflicts of interest

The authors declare no conflict of interest.

Acknowledgements

References

1 A. S. Abu Lila, M. H. Abdallah, S. U. D. Wani, H. V. Gangadharappa, K. M. Younes, E.-S. Khafagy, T. M. Shehata and M. S. Soliman, *Colloids Surf., A*, 2021, **625**, 126971.

2 N. Azamjah, Y. Soltan-Zadeh and F. Zayeri, *Asian Pac. J. Cancer Prev.*, 2019, **20**, 2015–2020.

3 A. Moin, S. U. D. Wani, R. A. Osmani, A. S. Abu Lila, E. S. Khafagy, H. H. Arab, H. V. Gangadharappa and A. N. Allam, *Drug Delivery*, 2021, **28**, 1626–1636.

4 H. Sung, J. Ferlay, R. L. Siegel, M. Laversanne, I. Soerjomataram, A. Jemal and F. Bray, *Ca-Cancer J. Clin.*, 2021, **71**, 209–249.

5 M. Arnold, E. Morgan, H. Rumgay, A. Mafra, D. Singh, M. Laversanne, J. Vignat, J. R. Gralow, F. Cardoso, S. Siesling and I. Soerjomataram, *Breast*, 2022, **66**, 15–23.

6 I. Schlam and S. M. Swain, *npj Breast Cancer*, 2021, **7**, 56.

7 J. Yao, J. Liu, Y. Li, Q. Wu and Y. Yang, *Cancer Biol. Ther.*, 2018, **19**, 349–354.

8 L. Sitia, M. Sevieri, L. Signati, A. Bonizzi, A. Chesi, F. Mainini, F. Corsi and S. Mazzucchelli, *Cancers*, 2022, **14**, 2424.

9 D.-Y. Oh and Y.-J. Bang, *Nat. Rev. Clin. Oncol.*, 2020, **17**, 33–48.

10 S. Dhillon, *Clin. Drug Invest.*, 2019, **39**, 221–229.

11 M. Oliveira, L. Garrigós, J. D. Assaf, S. Escrivá-de-Romaní and C. Saura, *Expert Rev. Anticancer Ther.*, 2020, **20**, 731–741.

12 K. Feldinger and A. Kong, *Breast Cancer*, 2015, **7**, 147–162.

13 D. M. Collins, N. T. Conlon, S. Kannan, C. S. Verma, L. D. Eli, A. S. Lalani and J. Crown, *Cancers*, 2019, **11**, 737.

14 H. Ma, Y. Liu, Z. Miao, S. Cheng, Y. Zhu, Y. Wu, X. Fan, J. Yang, X. Li and L. Guo, *Drug Dev. Res.*, 2022, **83**, 1641–1653.

15 T. Gunasekaran, T. Haile, T. Nigusse and M. D. Dhanaraju, *Asian Pac. J. Trop. Biomed.*, 2014, **4**, S1–S7.

16 A. S. Lila, H. Kiwada and T. Ishida, *Biol. Pharm. Bull.*, 2014, **37**, 206–211.

17 S. Sim and N. K. Wong, *Biomed. Rep.*, 2021, **14**, 42.

18 K. V. M. S. Tej, A. Moin, D. V. Gowda, S. Anjali, G. Karunakar, N. P. Patel and S. S. Kamal, *J. Chem. Pharm. Res.*, 2016, **8**, 627–643.

19 S. R. Ji, C. Liu, B. Zhang, F. Yang, J. Xu, J. Long, C. Jin, D. L. Fu, Q. X. Ni and X. J. Yu, *Biochim. Biophys. Acta*, 2010, **1806**, 29–35.

20 N. Slepičková Kasálková, P. Slepička and V. Švorčík, *Nanomaterials*, 2021, **11**, 2368.

21 L. Tang, Q. Xiao, Y. Mei, S. He, Z. Zhang, R. Wang and W. Wang, *J. Nanobiotechnol.*, 2021, **19**, 423.

22 B. Singh, S. Lohan, P. S. Sandhu, A. Jain and S. K. Mehta, *Nanobiomater. Med. Imaging*, 2016, 455–478.

23 N. Mody, R. K. Tekade, N. K. Mehra, P. Chopdey and N. K. Jain, *AAPS PharmSciTech*, 2014, **15**, 388–399.

24 S. K. Soininen, P. Lehtolainen-Dalkilic, T. Karppinen, T. Puustinen, G. Dragneva, M. U. Kaikkonen, M. Jauhiainen, B. Allart, D. L. Selwood, T. Wirth, H. P. Lesch, A. M. Määttä, J. Mönkkönen, S. Ylä-Herttuala and M. Ruponen, *Eur. J. Pharm. Sci.*, 2012, **47**, 848–856.

25 M. Pulkkinen, J. Pikkarainen, T. Wirth, T. Tarvainen, V. Haapa-aho, H. Korhonen, J. Seppälä and K. Järvinen, *Eur. J. Pharm. Biopharm.*, 2008, **70**, 66–74.

26 W. Yang, Y. Cheng, T. Xu, X. Wang and L.-p. Wen, *Eur. J. Med. Chem.*, 2009, **44**, 862–868.

27 N. Ahmadi Nasab, H. Hassani Kumleh, M. Beygzadeh, S. Teimourian and M. Kazemzad, *Artif. Cells, Nanomed., Biotechnol.*, 2018, **46**, 75–81.

28 M. H. Darvishi, A. Nomani, M. Amini, M. A. Shokrgozar and R. Dinarvand, *Int. J. Pharm.*, 2013, **456**, 408–416.

29 A. S. Abu Lila, M. S. Soliman, H. C. Kiran, H. V. Gangadharappa, K. M. Younes, E.-S. Khafagy, T. M. Shehata, M. M. Ibrahim and M. H. Abdallah, *J. Drug Delivery Sci. Technol.*, 2021, **63**, 102499.

30 C. L. Lay, H. Q. Liu, H. R. Tan and Y. Liu, *Nanotechnology*, 2010, **21**, 065101.

31 T. A. Wani, A. H. Bakheit, M. A. Abounassif and S. Zargar, *Front. Chem.*, 2018, **6**, 47.

32 A. Moin, N. K. F. Roohi, S. M. D. Rizvi, S. A. Ashraf, A. J. Siddiqui, M. Patel, S. M. Ahmed, D. V. Gowda and M. Adnan, *RSC Adv.*, 2020, **10**, 34869–34884.

33 E. A. Orellana and A. L. Kasinski, *Bio-Protoc.*, 2016, **6**, e1984.

34 A. Kordzadeh, S. Amjad-Iranagh, M. Zarif and H. Modarress, *J. Mol. Graphics Modell.*, 2019, **88**, 11–22.

35 X. Wang, Y. Zhu, M. Chen, M. Yan, G. Zeng and D. Huang, *Adv. Colloid Interface Sci.*, 2019, **270**, 101–107.

36 L. Liang, Z. Zhang, Z. Kong, Y. Liu, J.-W. Shen, D. Li and Q. Wang, *J. Mol. Graphics Modell.*, 2016, **66**, 20–25.

37 M. Magid and L. Q. Al-Karam, *J. Phys.: Conf. Ser.*, 2021, **2114**, 012038.

38 T. L. do Amaral Montanheiro, F. H. Cristóvan, J. P. B. Machado, D. B. Tada, N. Durán and A. P. Lemes, *J. Mater. Res.*, 2015, **30**, 55–65.

39 U. Hani, M. Rahamathulla, R. A. M. Osmani, M. Y. Begum, S. Wahab, M. Ghazwani, A. A. Fatease, A. H. Alamri, D. V. Gowda and A. Alqahtani, *Polymers*, 2022, **14**, 2520.

40 V. C. Ursachi, G. Dodi, A. G. Rusu, C. T. Mihai, L. Verestiuc and V. Balan, *Molecules*, 2021, **26**, 3467.

41 P. S. Uttekar, S. H. Lakade, V. K. Beldar and M. T. Harde, *IET Nanobiotechnol.*, 2019, **13**, 688–696.

42 S. Botelho da Silva, M. Krolicka, L. A. M. van den Broek, A. E. Frissen and C. G. Boeriu, *Carbohydr. Polym.*, 2018, **186**, 299–309.

43 A. Khoshoei, E. Ghasemy, F. Poustchi, M.-A. Shahbazi and R. Maleki, *Pharm. Res.*, 2020, **37**, 160.

44 V. Vichai and K. Kirtikara, *Nat. Protoc.*, 2006, **1**, 1112–1116.

45 M. A. Badea, M. Balas, M. Prodana, F. G. Cojocaru, D. Ionita and A. Dinischiotu, *Pharmaceutics*, 2022, **14**, 469.

46 M. Mullooly, D. Conklin, P. M. McGowan, N. A. O'Brien, N. O'Donovan, D. J. Slamon, J. Crown, R. S. Finn and M. J. Duffy, *J. Clin. Oncol.*, 2015, **33**, 1099.

47 R. Rauti, M. Musto, S. Bosi, M. Prato and L. Ballerini, *Carbon*, 2019, **143**, 430–446.

48 S. Devi, M. Kumar, A. Tiwari, V. Tiwari, D. Kaushik, R. Verma, S. Bhatt, B. M. Sahoo, T. Bhattacharya, S. Alshehri, M. M. Ghoneim, A. O. Babalghith and G. E.-S. Batiha, *Front. Mater.*, 2022, **8**, 798440.

49 V. Karthika, P. Kaleeswarran, K. Gopinath, A. Arumugam, M. Govindarajan, N. S. Alharbi, J. M. Khaled, M. N. Al-anbr and G. Benelli, *Mater. Sci. Eng., C*, 2018, **90**, 589–601.

50 J. M. Tan, B. Saifullah, A. U. Kura, S. Fakurazi and M. Z. Hussein, *Nanomaterials*, 2018, **8**, 389.

51 A. A. Haroun, H. A. Amin and S. H. Abd El-Alim, *IRBM*, 2018, **39**, 35–42.

52 K. Kostarelos, L. Lacerda, G. Pastorin, W. Wu, S. Wieckowski, J. Luangsivilay, S. Godefroy, D. Pantarotto, J.-P. Briand, S. Muller, M. Prato and A. Bianco, *Nat. Nanotechnol.*, 2007, **2**, 108–113.

53 S. Brahmachari, M. Ghosh, S. Dutta and P. K. Das, *J. Mater. Chem. B*, 2014, **2**, 1160–1173.